Singularity-Free Adaptive Control for Uncertain Omnidirectional Mobile Robots

Jeng-Tze Huang
Institute of Digital Mechatronic Techonology
Chinese Culture University
55, Hwa-Kang Road, Yang-Ming-Shan
Taipei, Taiwan, R.O.C
Email:hzz4@faculty.pccu.edu.tw

Tran Van Hung
Institute of Digital Mechatronic Techonology
Chinese Culture University
55, Hwa-Kang Road, Yang-Ming-Shan
Taipei, Taiwan, R.O.C
Email:hungtv@ntu.edu.vn

***Abstract*—Issues of control designs for omnidirectional mobile robots with parametric uncertainty, including the location of the center of the mass and the electrical constants, are addressed. First, the Lagrange method is used for deriving the system dynamics. Next, a singularity-free adaptive linearizing control is proposed to tackle with such a task. It ensures the asymptotic tracking stability and avoidance of control singularity at the same time. Simulation is carried out to demonstrate the validity of the proposed design in the final.**

I. Introduction

Omnidirectional mobile robots, by definition, are mobile platforms with full mobility and hence can move in any direction without requiring any re-orientation. Owing to their great potential in a wide variety of industrial and daily-life applications, corresponding modeling and control designs are well documented in the literature nowadays [1], [2]. Ignoring the dynamical behaviors, PID controllers following speed commands from inverse kinematics are generally adopted in early designs [3]. It may lead to unsatisfactory tracking performances in high-speed applications. Under such circumstances, nonlinear dynamic control designs are required. Kalmár-Nagy *et. al.* derived a dynamic model and presented a near-optimal control scheme for an ideal three-wheel omnidirectional platform [4]. Williams *et. al.* built a model with friction and slip [5]. Kinematic modeling and tracking control designs of a general omnidirectional mobile robot, taking the actuator saturation into account, is presented in [6]. The paper [7] adopted robust neural network based sliding mode approach for the trajectory tracking of omnidirectional mobile manipulators. Despite these achievements, issues regarding misalignment of the geometrical and the mass centers and uncertainty in the drivers' parameters are seldom addressed so far.

Regarding the first issue, Huang and Tsai [8] proposed an FPGA-implemented robust adaptive controller for the trajectory tracking of omnidirectional mobile platforms. However, the upper bounds of the angular velocity and acceleration are required *a priori*, which are generally unavailable in practice. By using Newton's mechanics, the model derived in [9] alleviates such drawbacks and the proposed design therein ensures the asymptotic tracking stability and avoided the control singularity at the same time. However, the translational friction appears as the disturbance in the derived model, which is not quite accurate. Besides, the robust control component uses higher control force than required, i.e., not essentially efficient. Regarding this, a new derivation based on Lagrange method is presented in this paper. Moreover, a slight modification of the control algorithm in [9] is given here to conquer the second drawback mentioned above.

The remainder of the paper is organized as follows: a derivation of the system's dynamical model based on the Lagrange method is presented in Section II. The central part of this paper, namely, the control design, is detailed in Section III. Simulation results on an omnidirectional robots with different driving motor characteristics are given in Section IV to demonstrate the usefulness of the proposed designs. Conclusion is finally drawn in Section V.

A. Preliminaries

Throughout this paper, $|\cdot|$ represents the absolute value of a real number, $\|\cdot\|$ is the 2-norm of a vector, S_θ and S_θ represent $\sin(\theta)$ and $\cos(\theta)$, respectively. Let $\xi, \alpha \in R^m$. The following operations are encountered frequently in this paper

$$\begin{aligned} \xi * \alpha &\triangleq [\xi_1\alpha_1, \cdots, \xi_m\alpha_m]^T, \\ \xi^{-1} &\triangleq [1/\xi_1, 1/\xi_2, \cdots, 1/\xi_m]^T \end{aligned} \tag{1}$$

II. Omnidirectional Mobile Robot

This section introduces the kinematics and dynamics of an omnidirectional mobile platform with three independent driving wheels equally spaced at 120 degrees apart. A 3-D plot of such a system is given in Fig. 1. In contrast to the one in [8], the dynamical model here groups all the acceleration-dependent uncertainty into the inertia matrix and therefore requires no robust control component for taking care of it.

A. Kinematics

For describing the planar motion of a mobile platform, as shown in Fig. 2, two coordinate frames are generally required. First, a moving frame $\{O_1, X_1, Y_1\}$ located at the reference point P of the cart (the geometrical center in this case) and a stationary world frame $\{O_0, X_0, Y_0\}$. The motion of the system can then be completely determined by specifying the

978-1-4673-5769-2/13/$31.00 ©2013 IEEE

coordinate (x_p, y_p) of the reference point P with respect to the world frame and the orientation θ of the cart with respect to the axis X_0. In the sequel, denote $\xi = [\xi_1\, \xi_2\, \xi_3]^T = [x_p\, y_p\, \theta]^T$.

By assumption, the center of mass P_c does not coincide with the geometrical center and its coordinate in the frame $\{O_0, X_0, Y_0\}$, denoted by $[x_c, y_c]^T$, is given by

$$\begin{bmatrix} x_c \\ y_c \end{bmatrix} = \begin{bmatrix} \xi_1 + dC_{\theta+\phi} \\ \xi_2 + dS_{\theta+\phi} \end{bmatrix} \tag{2}$$

where d is the distance between the points P and P_c, ϕ is the corresponding angle measured from X_1, By a direct differentiation, it yields

$$\begin{aligned} \begin{bmatrix} \dot{x}_c \\ \dot{y}_c \end{bmatrix} &= \begin{bmatrix} \dot{\xi}_1 - dS_{\theta+\phi}\dot{\theta} \\ \dot{\xi}_2 + dC_{\theta+\phi}\dot{\theta} \end{bmatrix} \\ \begin{bmatrix} \ddot{x}_c \\ \ddot{y}_c \end{bmatrix} &= \begin{bmatrix} \ddot{\xi}_1 - dC_{\theta+\phi}\dot{\theta}^2 - dS_{\theta+\phi}\ddot{\theta} \\ \ddot{\xi}_2 - dS_{\theta+\phi}\dot{\theta}^2 + dC_{\theta+\phi}\ddot{\theta} \end{bmatrix} \end{aligned} \tag{3}$$

The non-slip condition states that the velocities of at the contact points between the wheels and the surfaces must be zero, which lead to the following three constraint equations, [4]

$$[-S_{\alpha_i}\, C_{\alpha_i}\, l]R(\theta)\dot{\xi} + r\dot{\varphi}_i = 0, \quad i = 1, 2, 3, \tag{4}$$

where α_i is the angle between the position vector of the axis of the i'th wheel and the x-axis, and $R(\theta)$ is the rotation matrix given by

$$R(\theta) \triangleq \begin{bmatrix} C_\theta & S_\theta & 0 \\ -S_\theta & C_\theta & 0 \\ 0 & 0 & 1 \end{bmatrix} \tag{5}$$

The three constraint equations (4) can be written in a matrix form as

$$J_1 R(\theta)\dot{\xi} + J_2\dot{\varphi} = 0 \tag{6}$$

with

$$J_1 = \begin{bmatrix} 0 & 1 & l \\ -\frac{\sqrt{3}}{2} & -\frac{1}{2} & l \\ \frac{\sqrt{3}}{2} & -\frac{1}{2} & l \end{bmatrix} \tag{7}$$

and $J_2 = diag(r)$. Therefore, the inverse kinematics is given by

$$\begin{bmatrix} \omega_1 \\ \omega_2 \\ \omega_3 \end{bmatrix} = r^{-1}H(\theta) \begin{bmatrix} \dot{\xi}_1 \\ \dot{\xi}_2 \\ \dot{\theta} \end{bmatrix} \tag{8}$$

with

$$H(\theta) = \begin{bmatrix} S_\theta & -C_\theta & -l \\ S_{\theta+\frac{2\pi}{3}} & -C_{\theta+\frac{2\pi}{3}} & -l \\ S_{\theta-\frac{2\pi}{3}} & -C_{\theta-\frac{2\pi}{3}} & -l \end{bmatrix}, \tag{9}$$

where l is the distance from the geometric center P to the wheel axle, r and $\omega_i, i = 1, 2, 3$ are the radius and the angular velocities of the wheels, respectively. It is noted that $H(\theta)$ is nonsingular for all $\theta \in R$ and hence is always invertible. In fact, by a direct calculation, we have

$$H^{-1} = \frac{2\sqrt{3}}{9l} \begin{bmatrix} \sqrt{3}lS_\theta & \sqrt{3}lS_{\theta+\frac{2\pi}{3}} & \sqrt{3}lS_{\theta-\frac{2\pi}{3}} \\ -\sqrt{3}lC_\theta & -\sqrt{3}lC_{\theta+\frac{2\pi}{3}} & -\sqrt{3}lC_{\theta+\frac{2\pi}{3}} \\ -\frac{\sqrt{3}}{2} & -\frac{\sqrt{3}}{2} & -\frac{\sqrt{3}}{2} \end{bmatrix} \tag{10}$$

B. Dynamics

The Lagrange equations are generally used for deriving the dynamics of constraint mechanical systems. In this case , they can be described by the following two sets of differential equations [10]

$$\begin{aligned} \frac{d}{dt}(\frac{\partial T}{\partial \dot{\xi}}) - \frac{\partial T}{\partial \xi} &= R^T(\theta)J_1^T\lambda, \\ \frac{d}{dt}(\frac{\partial T}{\partial \dot{\varphi}}) - \frac{\partial T}{\partial \varphi} &= J_2^T\lambda + \tau_\varphi, \end{aligned} \tag{11}$$

where λ is the Lagrange coefficients associated with the constraints (6), τ_φ is the torques for the rotation of the wheels, and T is the total kinematic energy of the system given by

$$\begin{aligned} T &= \frac{1}{2}(m\dot{x}_c^2 + m\dot{y}_c^2 + J\dot{\theta}^2) \\ &= \frac{1}{2}[m(\dot{\xi}_1 - dS_{\theta+\phi}\dot{\theta})^2 \\ &\quad + m(\dot{\xi}_2 + dC_{\theta+\phi}\dot{\theta})^2 + J\dot{\theta}^2]. \end{aligned} \tag{12}$$

Assume that the dynamics of the wheels are negligible comparing to the dynamics of the platform, then the right-hand side of the second equation in (11) can be set to zero, leading to

$$\lambda = -\frac{1}{r}\tau_\varphi \tag{13}$$

By a direct calculation, we have

$$\begin{aligned} \frac{\partial T}{\partial \dot{\xi}_1} &= m(\dot{\xi}_1 - dS_{\theta+\phi}\dot{\theta}) \\ \frac{\partial T}{\partial \dot{\xi}_2} &= m(\dot{\xi}_2 + dC_{\theta+\phi}\dot{\theta}) \\ \frac{\partial T}{\partial \dot{\theta}} &= [m(\dot{\xi}_1 - dS_{\theta+\phi}\dot{\theta})(-dS_{\theta+\phi}) \\ &\quad + m(\dot{\xi}_2 + dC_{\theta+\phi}\dot{\theta})(dC_{\theta+\phi}) + J\dot{\theta}] \end{aligned} \tag{14}$$

and

$$\frac{\partial T}{\partial \theta} = -mdC_{\theta+\phi}\dot{\xi}_1\dot{\theta} - mdS_{\theta+\phi}\dot{\xi}_2\dot{\theta} \tag{15}$$

By substituting (14) and (15) into (11), after some manipulation, it yields

$$\mathcal{M}\ddot{\xi} + \mathcal{V}\dot{\xi} = \frac{1}{r}H^T(\theta)\tau_\varphi \tag{16}$$

where

$$\begin{aligned} \mathcal{M} &= \begin{bmatrix} m & 0 & -mdS_{\theta+\phi} \\ 0 & m & mdC_{\theta+\phi} \\ -mdS_{\theta+\phi} & mdC_{\theta+\phi} & J + md^2 \end{bmatrix} \\ \mathcal{V} &= \begin{bmatrix} 0 & 0 & -mdC_{\theta+\phi}\dot{\theta} \\ 0 & 0 & -mdS_{\theta+\phi}\dot{\theta} \\ 0 & 0 & 0 \end{bmatrix} \end{aligned} \tag{17}$$

The torque τ_i and the driving voltage u_i for a DC motor is generally related in a way of [4]

$$\tau_i = a_i u_i - b_i \omega_i, \quad i = 1, 2, 3 \tag{18}$$

where a_i and b_i are the proportional constants.

Define $u = [u_1\, u_2\, u_3]^T$ and

$$I_a = \begin{bmatrix} a_1 & 0 & 0 \\ 0 & a_2 & 0 \\ 0 & 0 & a_3 \end{bmatrix}, \quad I_b = \begin{bmatrix} b_1 & 0 & 0 \\ 0 & b_2 & 0 \\ 0 & 0 & b_3 \end{bmatrix}. \tag{19}$$

The dynamical equations (17) can now be written in a compact form of

$$\mathcal{M}\ddot{\xi} + [\mathcal{V} + \frac{1}{r^2} H^T I_b H]\dot{\xi} = \frac{1}{r} H^T I_a u \tag{20}$$

Finally, it is easy to verify that the following two properties, which hold for a general robot, also hold in this application.

- *P1):* $\mathcal{M}$ is always symmetric positive definite for all values of θ.
- *P2):* the matrix $\dot{\mathcal{M}} - 2\mathcal{V}$ is skew symmetric.

III. Control Designs

With the uncertainty in the system parameters in m, J, d, ϕ, a_i and $b_i, i = 1, 2, 3$, the objective here is to synthesize a control law for u_i, such that the position vector $\xi(t)$ tracks the reference trajectory $\xi_d(t)$ with high accuracies. As can be seen from (20), the matrix I_a affine with the control input is unknown and hence can not be canceled out directly. The switching based control approach, mainly consisting of an adaptive linearizing control plus a robust controller activated only when near the singularity, is adopted here for attaining the objectives [11].

Given a desired trajectory vector $\xi_d(t)$, the tracking error vector is

$$e(t) = \xi(t) - \xi_d(t) \tag{21}$$

The sliding surface in the phase plane is defined as

$$S = \dot{e} + \Lambda e = 0, \tag{22}$$

where $\Lambda > 0$ is the gain matrix at disposal.

The system dynamics can be written in terms of S as

$$\mathcal{M}\dot{S} = \frac{1}{r} H^T(\theta) I_a u - \mathcal{V} S + Y\vartheta \tag{23}$$

where $\psi = [\psi_1, \psi_2, \psi_3]^T = -\dot{\xi}_d + \Lambda e$, $\vartheta = [m, J + md^2, mdC_\phi, mdS_\phi, b_1, b_2, b_3]^T \in R^7$ and $Y \in R^{3\times 7}$ is the corresponding regressor such that

$$Y\vartheta = -\mathcal{M}\dot{\psi} + \mathcal{V}\psi - \frac{1}{r^2} H^T I_b T \dot{\xi} \tag{24}$$

Remark 1: Since $x^T H^T(\theta) I_a H(\theta) x = ||I_a^{1/2} H(\theta) x||^2, \forall x \in R^3$ and $H(\theta)$ is nonsingular for all $\theta \in R$, therefore, the matrix $H^T(\theta) I_a H(\theta)$ is positive definite for all $\theta \in R$. Consequently, there exists a positive constant λ_0, such that

$$\lambda_0 ||x||^2 \le x^T H^T(\theta) I_a H(\theta) x, \forall x \in R^3. \tag{25}$$

Such a property ensures the controllability of the system and, in the upcoming design, λ_0 is assumed known *a priori*.

It is clear that stabilization of the dynamics in (23) ensures the asymptotic convergence of the tracking errors $e(t)$ to zero. The parametric uncertainty appeared in the right-hand side has to be handled first. The adaptive linearizing control approach arises naturally under such circumstances. However, the so-called control singularity could happen when the estimated inverse of the matrix affine with the control input becomes singular. To counteract such a drawback, the hybrid control approach in [11] is adopted.

First the switching function $\rho(x)$ is recalled here

$$\rho(x) \triangleq 1 - \exp[-(x/\delta)^2], \tag{26}$$

where $\delta > 0$ is the corresponding transition width at disposal. It possesses the following useful properties

- *P3):* $0 \le \rho(x) \le 1, \quad \forall x \in R$;
- *P4):* $\rho(x)/x \to 0$, as $x \to 0$;
- *P5):* $\rho(x) \to 1$, as $x \to \infty$;
- *P6):* the value $\max_{x\neq 0} \rho(x)/x$ is bounded.

The proposed control algorithm can now be specified as follows

$$u = u_a + u_r, \tag{27}$$

where

$$\begin{aligned} u_a &= -r\bar{\rho}(t) * [(HS) * \hat{a}]^{-1} * S * [k_s S + Y\hat{\vartheta}], \\ u_r &= -\frac{r}{\lambda_0}(k_s + \frac{||Y\hat{\vartheta}||}{||S||})||\bar{I} - \bar{\rho}||HS, \end{aligned} \tag{28}$$

with k_s being the gain constant, $\bar{I} = [1\,1\,1]^T$, $\hat{(\cdot)}$ being the estimation of $(\cdot)$, and

$$\bar{\rho}(t) = [\rho((HS)_1\hat{a}_1), \rho((HS)_2\hat{a}_2), \rho((HS)_3\hat{a}_3)]^T. \tag{29}$$

The corresponding update algorithms for $\hat{\vartheta}(t)$ and $\hat{a}_i$ are given by

$$\begin{aligned} \dot{\hat{a}} &= -\Gamma_a[\bar{\rho} * (HS)] * [(HS) * \hat{a}]^{-1} * S * (k_s S + Y\hat{\vartheta}), \\ \dot{\hat{\vartheta}} &= \Gamma_\theta Y^T S, \end{aligned} \tag{30}$$

where Γ_a and Γ_θ are the tuning gains, and $\hat{a} = [\hat{a}_1\, \hat{a}_2\, \hat{a}_3]^T$.

The main contribution of this paper is summarized as follows

Theorem 1: Consider the closed-loop system, consisting of the error dynamics in (23), the control in (27), and the update algorithm in (30). If the value λ_0 is known *a priori*, then

- *T1):* all the signals in the closed-loop system remain bounded $\forall t \ge 0$;
- *T2):* the tracking error $e(t) \to 0$ as $t \to \infty$.

Proof:

Select the following Lyapunov function

$$V(t) \triangleq \frac{1}{2}(S^T \mathcal{M} S + \tilde{a}^T \Gamma_a^{-1} \tilde{a} + \tilde{\vartheta}^T \Gamma_\theta^{-1} \tilde{\vartheta}). \tag{31}$$

where $\tilde{(\cdot)} = \hat{(\cdot)} - (\cdot)$ being the estimation error.

The time derivative of $V(t)$, taking (28)-(30) into account, can be calculated as follows

$$\begin{aligned}\dot{V}(t) &= S^T\mathcal{M}\dot{S}+\frac{1}{2}S^T\dot{\mathcal{M}}S+\tilde{a}^T\Gamma_a^{-1}\dot{\hat{a}}+\tilde{\vartheta}^T\Gamma_\theta^{-1}\dot{\hat{\vartheta}}\\ &= S^T[\frac{1}{r}T^T(\theta)I_au-\mathcal{V}S+Y\vartheta]+\frac{1}{2}S^T\dot{\mathcal{M}}S\\ &\quad+\tilde{a}^T\Gamma_a^{-1}\dot{\hat{a}}+\tilde{\vartheta}^T\Gamma_a^{-1}\dot{\hat{\vartheta}}\\ &= S^T[\frac{1}{r}T^T(\theta)I_au+Y\hat{\vartheta}-Y\tilde{\vartheta}]\\ &\quad+\frac{1}{2}S^T(\dot{\mathcal{M}}-2\mathcal{V})S+\tilde{a}^T\Gamma_a^{-1}\dot{\hat{a}}+\tilde{\vartheta}^TY^TS \quad (32)\end{aligned}$$

By invoking P2), (32) can be written as

$$\begin{aligned}\dot{V}(t) &= -k_sS^TS+S^T[\frac{1}{r}H^T(\theta)I_au_a\\ &\quad+\bar{\rho}*(k_sS+Y\hat{\vartheta})]+S^T[\frac{1}{r}H^T(\theta)I_au_r\\ &\quad+(\bar{I}-\bar{\rho})*(k_sS+Y\hat{\vartheta})]+\tilde{a}^T\Gamma_a^{-1}\dot{\hat{a}} \quad (33)\end{aligned}$$

Noting that

$$\begin{aligned}\frac{1}{r}S^TH^TI_au_a &= \frac{1}{r}[(HS)*a]^Tu_a\\ &= -\bar{\rho}^T[(HS)*a]*[(HS)*\hat{a}]^{-1}\\ &\quad*S*(k_sS+Y\hat{\vartheta})\\ &= -\bar{\rho}^TS*(k_sS+Y\hat{\vartheta})+\tilde{a}^T[\bar{\rho}*(HS)]\\ &\quad*[(HS)*\hat{a}]^{-1}*S*(k_sS+Y\hat{\vartheta})\\ &= -S^T\bar{\rho}*(k_sS+Y\hat{\vartheta})-\tilde{a}^T\Gamma_a^{-1}\dot{\hat{a}} \quad (34)\end{aligned}$$

and

$$\begin{aligned}\frac{1}{r}S^TH^TI_au_r &= -\frac{S^TH^TI_aHS}{\lambda_0}||\bar{I}-\bar{\rho}||(k_s+\frac{||Y\hat{\vartheta}||}{||S||})\\ &\leq -||\bar{I}-\bar{\rho}||(k_sS^TS+||Y\hat{\vartheta}||||S||). \quad (35)\end{aligned}$$

Therefore, by substituting (34)-(35) into (33), it yields

$$\dot{V}(t) \leq -k_sS^TS \quad (36)$$

The Lyapunov function $V(t)$ is thus nonincreasing and therefore $V(\infty)$ is well defined since $V(t)$ is lower-bounded. It follows immediately that S, $\tilde{\vartheta}$, and $\tilde{I}_a$ are bounded, which in turn implies the boundedness of e, $\hat{\vartheta}$, and $\hat{I}_a$ by definitions. Next, by integrating (36) from 0 to ∞, it can be seen that the signal $S(t)$ is L_2-bounded, which, together with the fact of $\dot{S}(t)$ being uniformly bounded, implies its convergence to zero as $t\to\infty$ from Barbalat's lemma. It follows immediately that the tracking error $e(t)$ will converge to zero asymptotically. ■

Remark 2: As is well known, the sign function appearing in (28) can be replaced with the saturation function to eliminate the possible chattering behavior [12].

IV. Simulation

Simulation study is carried out in this section to demonstrate the validity of the proposed design.

The adopted numerical values in this simulation are $m=8.0kg, J=14.0kgm^2, r=0.08m, l=0.3m, d=0.15m, \delta=0.1, a_1=0.1, a_2=0.2, a_3=0.3, b_1=0.2, b_2=0.1, b_3=0.15, \lambda_0=0.1, \Lambda=2I_,, \phi=\pi/4, k_s=2.0$. The desired trajectory is a circle given by $q_d=0.5[\cos(0.2t),\sin(0.2t),0]^t$. The initial state of the wheeled robot is chosen as $[P_0(0)\,\dot{P}_0(0)]^t=[0.2\,0.3\,0.1\,0.0\,0.1\,0.2]^T$.

The tracking errors converge asymptotically to zero, as can be seen in Fig. 3. To highlight the main achievement of our design, the calculated driving voltages of the proposed design and a pure linearizing adaptive control, are depicted in Fig. 4 and Fig. 5, respectively. As can be seen, the control singularity phenomenon has been suppressed by our scheme.

V. Conclusion

We have constructed a singularity-free adaptive controller for the uncertain omnidirectional mobile robot system under the dynamical parameters, including the electrical ones in the motor driving circuits. The proposed design ensures the asymptotical tracking stability and avoids the control singularity at the same time.

References

[1] F. G. Pin and S. M. Killough, "A new family of omnidirectional and holonomic wheeled platforms for mobile robots," *IEEE Trans. Rob. Automat.,* vol. 10, no. 4, pp. 480-489, 1994.

[2] A. S. Conceiqão, A. P. Moreira, and P. J. Costa, "Practical approach of modeling and parameters estimation for omnidirectional mobile robots," *IEEE Trans. Mechatronics,* vol. 14, no. 3, pp. 377-381, 2009.

[3] I. E. Paromtchik and U. Rembold, "A practical approach to motion generation and control for an omnidirectional mobile robot," in *Proc. the 1994 IEEE Int. Conf. Robotics and Automation,* vol. 4, pp. 2790 - 2795.

[4] T. Kalmár-Nagy, R. D'Andrea, and P. Gauguly, "Near-optimal dynamic trajectory generation and control of an omnidirectinal vehicle," *Robot. Autom. Syst.*, vol. 46, no. 1, pp. 47-64, 2004.

[5] R. L. Williams, B. E. Carter, P. Gallina and G. Rosati, "Dynamic model with slip for wheeled omnidirectional robots," *IEEE Trans. Robot. Automat.,* vol. 18, no. 3, pp. 285-293, 2002.

[6] G. Indiveri, "Swedish wheeled omnidirectional mobile robots: kinematic analysis and control," *IEEE Trans. Rob. Automat.,* vol. 25, no. 1, pp. 164-171, 2009.

[7] D. Xu, D.-B Zhao, J.-Q. Yi, X.-M. Tan, "Trajectory tracking control of omnidirectional wheeled mobile manipulators: robust neural network-based sliding mode approach," *IEEE Trans. Syst. Man. & Cybern.,* vol. 39, no. 3, pp. 788-799, 2009.

[8] H. -C. Huang and C. -C. Tsai, "FPGA implementation of an embedded robust adaptive controller for autonomous omnidirectional mobile platform", *IEEE Trans. Ind. Electronics,* vol. 56, no. 5, pp. 1604-1616, 2009.

[9] J.-T. Huang and C.-H. Chang, "A composite controller for uncertain omnidirectional mobile robots," 2011 8'th Asian Control Conference, pp. 777-781, May. 15-18, 2011.

[10] G. Campion, G. Bastin, B. D'Andréa-Novel, "Structural properties and classification of kinematic and dynamic models of wheeled mobile robots,," *IEEE Trans. Robot. Automat.,* vol. 12, no. 1, pp. 47-62, 1996.

[11] J. T. Huang and Y. M. Chen, "A smooth switching adaptive controller for linearizable systems with improved transient performance," *Int. J. Adaptive Contr. Signal Processing,* vol. 20, no. 9, pp. 431-446, 2006.

[12] J.-J. E. Slotine and J. A. Cortsee, "Adaptive sliding controller synthesis for nonlinear systems," *Int. J. Contr.,* vol. 43, no. 6, pp. 1631-1651, 1986.

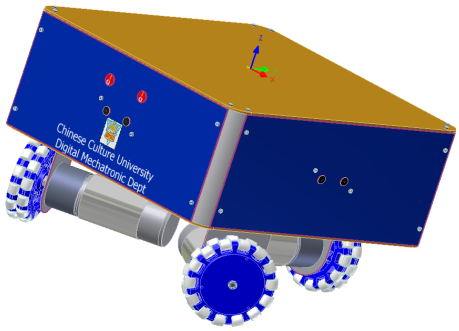

Fig. 1 3-D view of an omnidirectional mobile robot

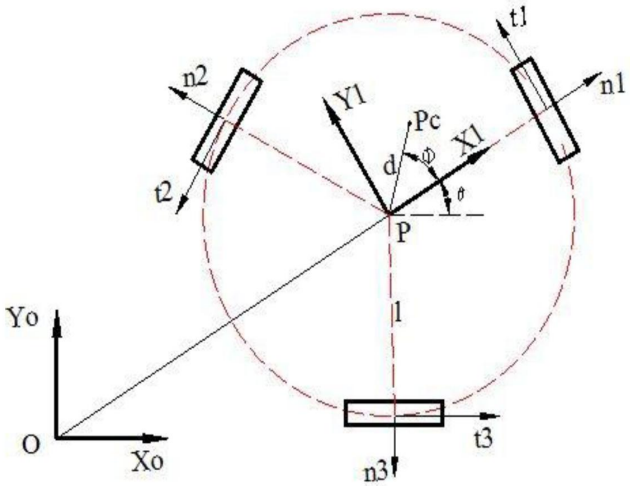

Fig. 2 Coordinate system

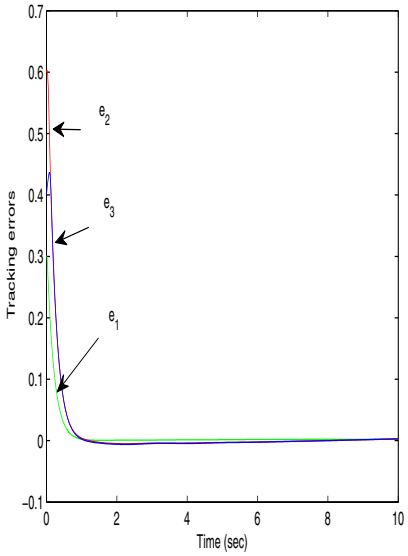

Fig. 3 Tracking error trajectories

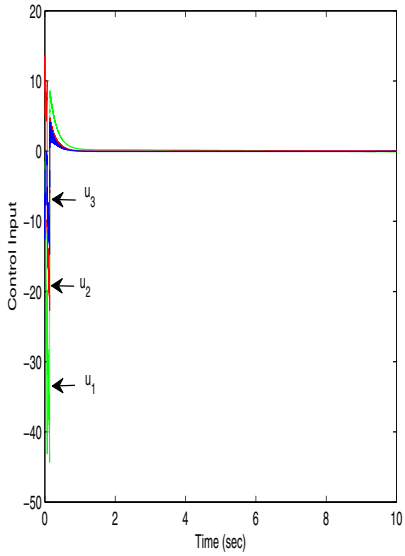

Fig. 4 Driving voltages of the proposed design

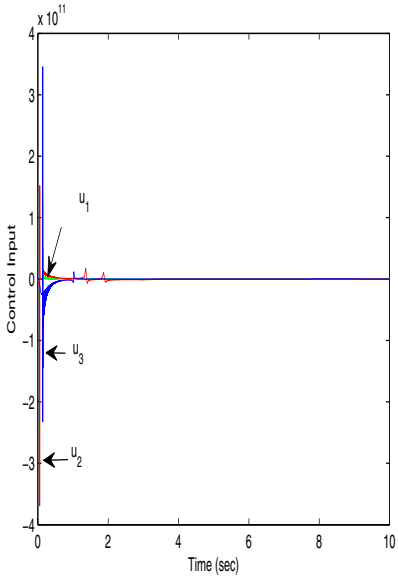

Fig. 5 Driving voltages of pure adaptive control